



OPEN

SUBJECT AREAS:

CARBOHYDRATE
CHEMISTRY

ELECTRONIC DEVICES

Received

7 February 2014

Accepted

2 June 2014

Published

17 June 2014

Correspondence and requests for materials should be addressed to H.O. (hokamoto@cc.okayama-u.ac.jp) or Y.K. (kubozono@cc.okayama-u.ac.jp)

An Extended Phenacene-type Molecule, [8]Phenacene: Synthesis and Transistor Application

Hideki Okamoto¹, Ritsuko Eguchi², Shino Hamao², Hidenori Goto², Kazuma Gotoh¹, Yusuke Sakai², Masanari Izumi², Yutaka Takaguchi³, Shin Gohda⁴ & Yoshihiro Kubozono^{2,5,6}

¹Department of Chemistry, Okayama University, Okayama 700-8530, Japan, ²Research Laboratory for Surface Science, Okayama University, Okayama 700-8530, Japan, ³Graduate School of Environmental and Life Science, Okayama University, Okayama 700-8530, Japan, ⁴NARD Co. Ltd., Amagasaki 660-0805, Japan, ⁵Research Centre of New Functional Materials for Energy Production, Storage and Transport, Okayama University, Okayama 700-8530, Japan, ⁶Japan Science and Technology Agency, ACT-C Kawaguchi 322-0012, Japan.

A new phenacene-type molecule, [8]phenacene, which is an extended zigzag chain of coplanar fused benzene rings, has been synthesised for use in an organic field-effect transistor (FET). The molecule consists of a phenacene core of eight benzene rings, which has a lengthy π -conjugated system. The structure was verified by elemental analysis, solid-state NMR, X-ray diffraction (XRD) pattern, absorption spectrum and photoelectron yield spectroscopy (PYS). This type of molecule is quite interesting, not only as pure chemistry but also for its potential electronics applications. Here we report the physical properties of [8]phenacene and its FET application. An [8]phenacene thin-film FET fabricated with an SiO₂ gate dielectric showed clear p-channel characteristics. The highest μ achieved in an [8]phenacene thin-film FET with an SiO₂ gate dielectric is 1.74 cm² V⁻¹ s⁻¹, demonstrating excellent FET characteristics; the average μ was evaluated as 1.2(3) cm² V⁻¹ s⁻¹. The μ value in the [8]phenacene electric-double-layer FET reached 16.4 cm² V⁻¹ s⁻¹, which is the highest reported in EDL FETs based on phenacene-type molecules; the average μ was evaluated as 8(5) cm² V⁻¹ s⁻¹. The μ values recorded in this study show that [8]phenacene is a promising molecule for transistor applications.

Field effect transistors (FETs) using thin films or single crystals of phenacene-type molecules, which consist of a number of coplanar benzene rings fused into an extended W-shape configuration have shown excellent p-channel properties, with the field-effect mobility (μ) being greater than 1 cm² V⁻¹ s⁻¹^{1–11}. The highest μ values were achieved by [6]phenacene in a thin-film FET⁷, and for [7]phenacene in a single-crystal FET¹⁰. The μ value for the former FET reached 7.4 cm² V⁻¹ s⁻¹, while that for the latter reached 6.7 cm² V⁻¹ s⁻¹. Because of such excellent FET characteristics, FETs with phenacene-type molecules are of interest for their potential practical applications. Studies on interface control have been performed in these FETs because interface control is desirable between the source/drain electrodes and the active layer, and between the gate dielectric and the active layer, as a way to further improve their FET characteristics^{3,4,10,11}. We have also pursued a possible sensor application based on phenacene thin-film FETs because exposure to O₂ gas produced an increase in μ and absolute drain current ($|I_D|$) in some of the FET devices^{2,3,5,6,8}. The O₂ gas sensing effect is seen most strongly in an FET based on a thin film of picene (five benzene rings)^{2,3}. Thus, FET devices with phenacene-type molecules may be quite promising candidates for future electronics.

In the past five years we have systematically synthesised phenacene-type molecules from picene to [7]phenacene (seven benzene rings), including their derivatives^{1,12–14}, and investigated their structures and electronic properties as well as their FET characteristics. Their electronic structures did not significantly change despite the increase in the number of benzene rings¹³. This is due to the little-changed length of the long axis of the molecule, while the electronic structures clearly did change in acene-type molecules because of their changed length¹³. The crystal structures of these molecules are similar to each other (herringbone), although the defined axis directions are different in [6]phenacene from other molecules, picene and [7]phenacene^{1,6,8,10}. The *ab*-plane of the crystals of phenacene-type molecules grows parallel to the surface of SiO₂ (or other gate dielectrics), which is preferable for FET channel conduction because conduction occurs in the *ab*-plane^{9,10}. These desirable features guarantee high performance in FETs based on phenacene-type molecules.



The synthesis of phenacene molecules becomes difficult when the number of benzene rings increases because of the difficulty of dissolving the molecules in common solvents. Therefore, the study of the synthesis of phenacene molecules with a large number of benzene rings remains challenging, and few reports of the synthesis of phenacene molecules with more than seven benzene rings have appeared^{15–17}.

Recently, the acene-type molecule, hexacene (six benzene rings) was synthesised and its FET properties were characterised, showing a μ value as high as $4.28 \text{ cm}^2 \text{ V}^{-1} \text{ s}^{-1}$ ¹⁸. This molecule was stable in the dark but highly vulnerable to photolysis in solution. In contrast, phenacene-type molecules are known to be more stable than acene-type molecules, and show no degradation under ambient conditions, even in the light^{1–13}. This implies that phenacenes are more suitable for FET application than acenes. Thus, the search for an effective synthetic route to phenacene molecules with more than seven benzene rings is significant from the viewpoint of pure chemistry and also for their potential application in practical electronics.

In this study, we have synthesised [8]phenacene, a molecule with eight benzene rings, and have clarified its physical properties and FET characteristics; the molecular structure is shown in Figure 1(a). The synthesis of this molecule was previously reported in a patent¹⁷, with the μ value in its thin-film FET reported to be $5.8 \times 10^{-2} \text{ cm}^2 \text{ V}^{-1} \text{ s}^{-1}$. The patent does not clearly show the details of the synthetic route, material characterisation and FET performance, but the synthetic route is clearly different from that adopted in this study. As described later, our synthetic route is quite effective and can produce a large amount of pure [8]phenacene. Furthermore, the features of the [8]phenacene molecule were clarified for the first time in this study using solid-state cross-polarization magic angle spinning (CP-MAS) NMR, optical absorption, X-ray diffraction (XRD) and atomic force microscopy (AFM). The FET characteristics of the [8]phenacene thin-film FET fabricated in this study are excellent, and the μ value in the [8]phenacene thin-film FET with an SiO_2 gate dielectric is higher by a factor of 30 than the $5.8 \times 10^{-2} \text{ cm}^2 \text{ V}^{-1}$ reported in the cited patent's data¹⁷. In particular, the performance of an FET with an electric-double-layer (EDL) capacitor is the best among the phenacene FETs fabricated so far, with a record μ of $16.4 \text{ cm}^2 \text{ V}^{-1} \text{ s}^{-1}$.

Results

Synthetic protocol for [8]phenacene. Mallory's homologation strategy^{15,16,19} was used in the synthesis of [8]phenacene, as shown in Figure 2. A Wittig reaction between (1-naphthylmethyl)-triphenylphosphonium chloride **1** and *o*-tolualdehyde **2** in the presence of KOH produced naphthyltolylethene **3**. The crude compound **3** containing *E*- and *Z*-isomers was used for the following photoreaction without separation of the isomers. Photocyclisation of compound **3** in the presence of iodine under aerated conditions produced 1-methylchrysene **4** (66% from **1** and **2**). Bromination of the methyl group of compound **4** with *N*-bromosuccinimide (NBS) in the presence of benzoylperoxide (BPO) produced 1-(bromomethyl)chrysene **5** (76%), and subsequent substitution with triphenylphosphine gave phosphonium salt **6** (93%). 1-Phenanthrenecarbaldehyde **8** was prepared by a Sommelet reaction²⁰ of 1-(bromomethyl)phenanthrene **7** (89%). A Wittig reaction of phosphonium salt **6** with aldehyde **8** produced chrysenylphenanthrylethene **9** (62%, a mixture of *E*- and *Z*-isomers) as a precursor to [8]phenacene. Finally, photoirradiation of compound **9** in the presence of iodine resulted in the formation of the desired [8]phenacene (28%).

Chrysenylphenanthrylethene **9**, which is a key synthetic intermediate in the production of [8]phenacene, was characterised by its conversion to the corresponding alkane **10** by catalytic hydrogenation of the double bond, because compound **9** prepared by the Wittig reaction contained *E*- and *Z*-isomers and it was poorly soluble in common organic solvents. The molecular structure of product **10**

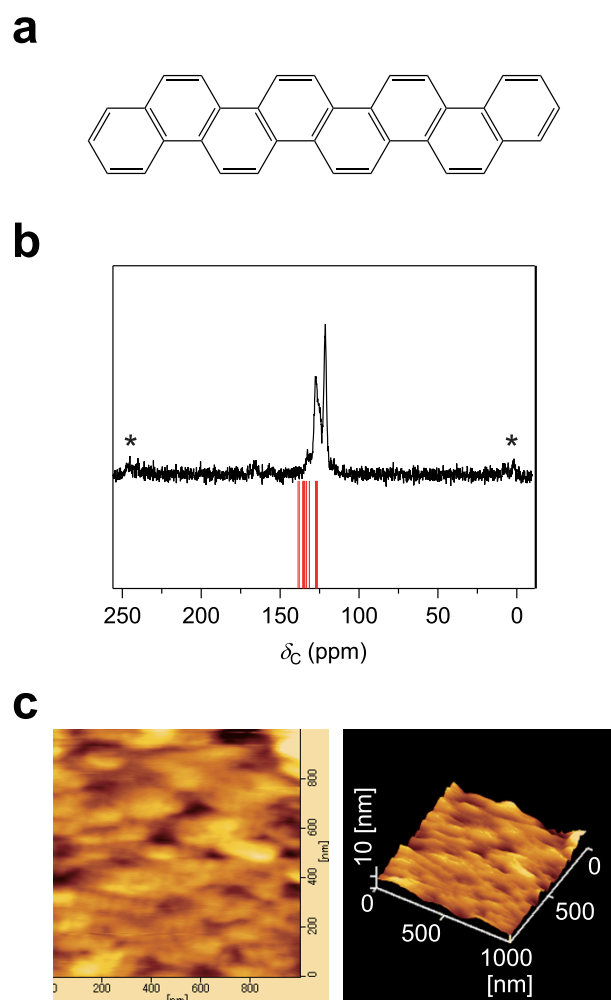


Figure 1 | (a) Molecular structure of [8]phenacene (H atoms omitted). (b) Solid state CP-MAS ^{13}C NMR spectra (125 MHz) of [8]phenacene (upper). Calculated ^{13}C chemical shifts at B3LYP/6-311+(2d,p)//B3LYP/6-31G level (lower). Asterisks denote spinning side bands. (c) AFM images of [8]phenacene thin film on SiO_2/Si substrate.

was identified by ^1H and ^{13}C NMR, fast atom bombardment high-resolution mass spectrometry (FAB HRMS) and elemental analysis, as described in the Methods section. Thus, we can conclude that intermediate **9** was in fact chrysenylphenanthrylethene (see Figure 2).

Here, we stress that a clear identification of intermediate **9** completely guarantees the successful production of [8]phenacene because the photocyclisation from **9** to [8]phenacene is an established and well-known reaction, the Mallory photocyclisation^{15,16,19,21}, which has been widely used for the preparation of picene, [6]phenacene, [7]phenacene and alkyl-substituted picene by our group²². Experimental details of each step in the synthesis of [8]phenacene are described in the Methods section and Supplementary Information.

Characterisation by energy dispersive X-ray spectroscopy, mass spectrum and elemental analysis. The spectrum from energy dispersive X-ray spectroscopy of an [8]phenacene sample is shown in Figure S1 in Supplementary information. The spectrum shows a pronounced peak for C with small peaks due to O, Al and Cu. These additional small peaks due to Al and Cu originate from the sample holder, and the peak due to O may be from the CuO of sample holder. No peaks due to iodine appear in the spectrum although iodine was used for catalysis in the synthesis of [8]phenacene as described in the synthesis protocol.

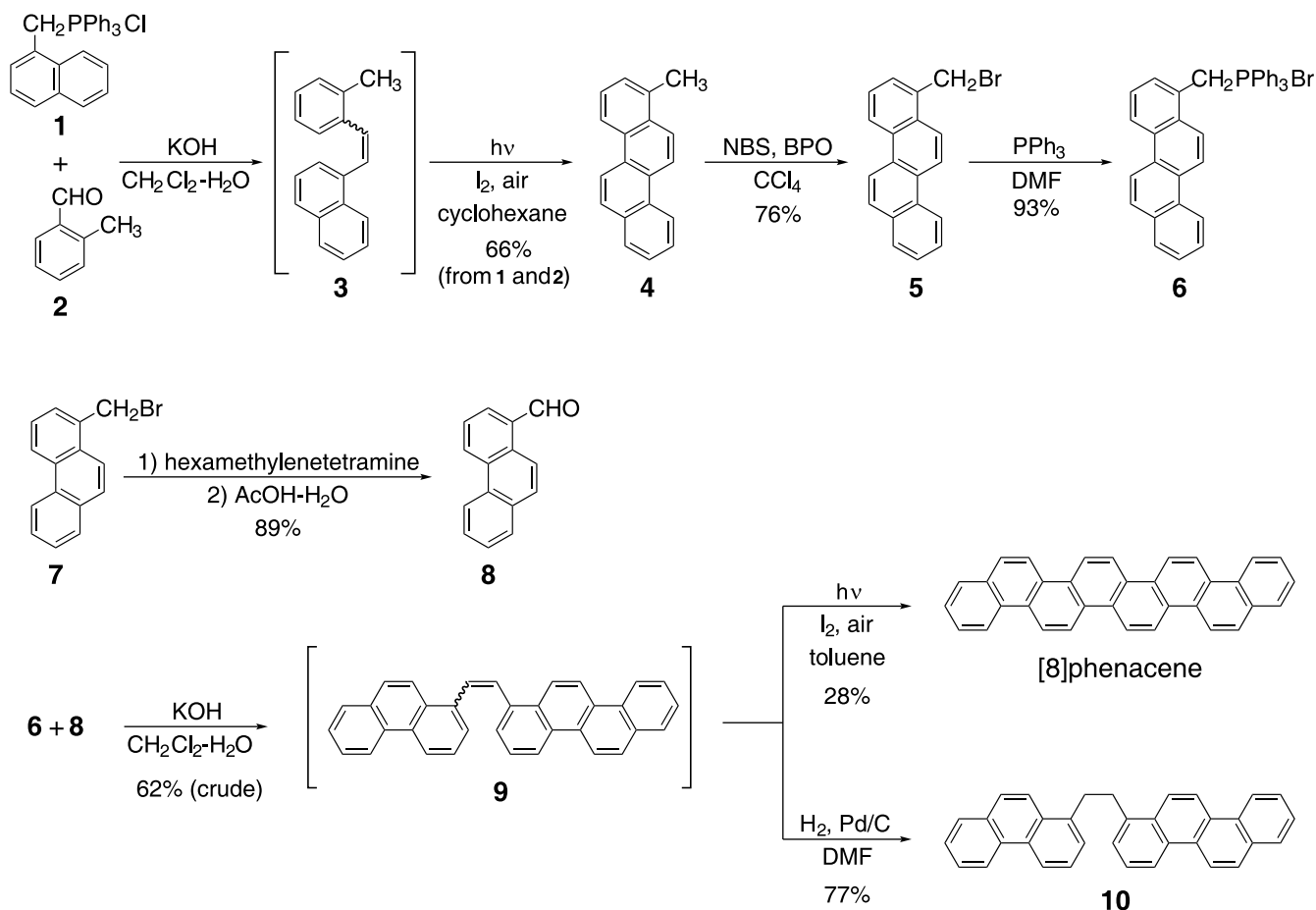


Figure 2 | Synthetic route to [8]phenacene.

The Matrix-Assisted Laser Desorption/Ionization Time-of-Flight Mass Spectrometry (MALDI-TOF MS) of $m/z = 428.146$ ([8]phenacene⁺) for [8]phenacene sample is consistent with the calculated value ($m/z = 428.157$) (see Figure S2 in Supplementary information). Elemental analysis of [8]phenacene is as follows: C: 95.30%; H: 4.70% (calculated), C: 95.04%; H: 4.51% (experimental). Thus, the elemental analysis also shows good agreement between calculated and experimental values. These data support the successful synthesis of [8]phenacene.

Solid state CP-MAS NMR analysis. The NMR spectrum of a solution of [8]phenacene could not be observed due to its poor solubility in common organic solvents. Therefore, the characterisation of [8]phenacene was undertaken using solid-state CP-MAS ¹³C NMR spectroscopy (Figure 1(b)). The [8]phenacene sample displayed ¹³C NMR peaks at chemical shifts, δ , of 121.4, 127.6 and \sim 130 (broad) ppm. In order to assign the signals, the ¹³C chemical shifts of [8]phenacene were calculated by density function theory (DFT) at the B3LYP/6-311+(2d,p)//B3LYP/6-31G level; details are shown in Supplementary information. As seen in Figure 1(b), the calculated ¹³C chemical shifts substantially reproduce the experimental NMR peaks. Actually, the calculated ¹³C chemical shifts slightly overestimate the experimental ones. Similar overestimation in calculated peaks is found for hexacene¹⁸, and is generally found in this level's calculation. Consequently, we concluded that the observed ¹³C signals can be assigned to [8]phenacene.

Furthermore, we measured the solid-state CP-MAS ¹³C NMR of precursor **9** (see Figure 2), which showed ¹³C signals at a δ of 123.4, 126.2 and \sim 130 (broad) ppm (Figure S9 in Supplementary Information). The ¹³C NMR peaks of **9** appeared in a similar region to

those of [8]phenacene, but they showed a different spectral pattern from that shown in Figure 1(b), implying that the sample obtained in the final step of Figure 2 was successfully converted from **9** to [8]phenacene; spectra of **9** and [8]phenacene are both shown in Supplementary Information, as described in the Methods section. Thus, the NMR data support the identity of the sample as [8]phenacene.

Characterisation of [8]phenacene thin film by AFM and XRD.

Figure 1(c) shows the AFM images of [8]phenacene thin film formed on SiO₂/Si. The AFM image shows closely packed granules. The size of each granule is not clear, but the root mean square (rms) roughness of [8]phenacene thin film is evaluated as 1.7 nm, showing a flat surface as in picene (3.1 nm)⁴, [6]phenacene (6.0 nm)⁶, and [7]phenacene (4.8 nm)⁸ thin films.

XRD patterns of an [8]phenacene thin film formed on SiO₂/Si are shown in Figure 3(a). Only 00 l reflections are observed, in the same manner as picene⁴, [6]phenacene⁶, and [7]phenacene⁸, implying that the ab -planes (ab -layer) in a thin [8]phenacene film are parallel to substrate surface. The distance between layers substantially corresponds to the inter-plane spacing, $\langle d_{001} \rangle (=1/|c^*|$ where c^* is a reciprocal lattice of c), which is estimated to be 2.04(4) nm for SiO₂/Si from the 00 l reflections. From the similarity of the XRD pattern of [8]phenacene thin film to other phenacene thin films, the space group of [8]phenacene is assumed to be P2₁ (No. 4) as in picene^{23,24}, and the β is taken as 90°; herringbone stacking in the ab -layer is expected. Since the van der Waals length of the long axis of [8]phenacene is 2.18 nm, the inclination angle is estimated to be 20° with respect to c^* , which is the same as [7]phenacene (\sim 20°)⁸ and smaller than that of picene and [6]phenacene⁶ (\sim 30°); the inclination angle of picene was here evaluated to be \sim 30° using $1/|c^*| = 1.336$ nm (ref.

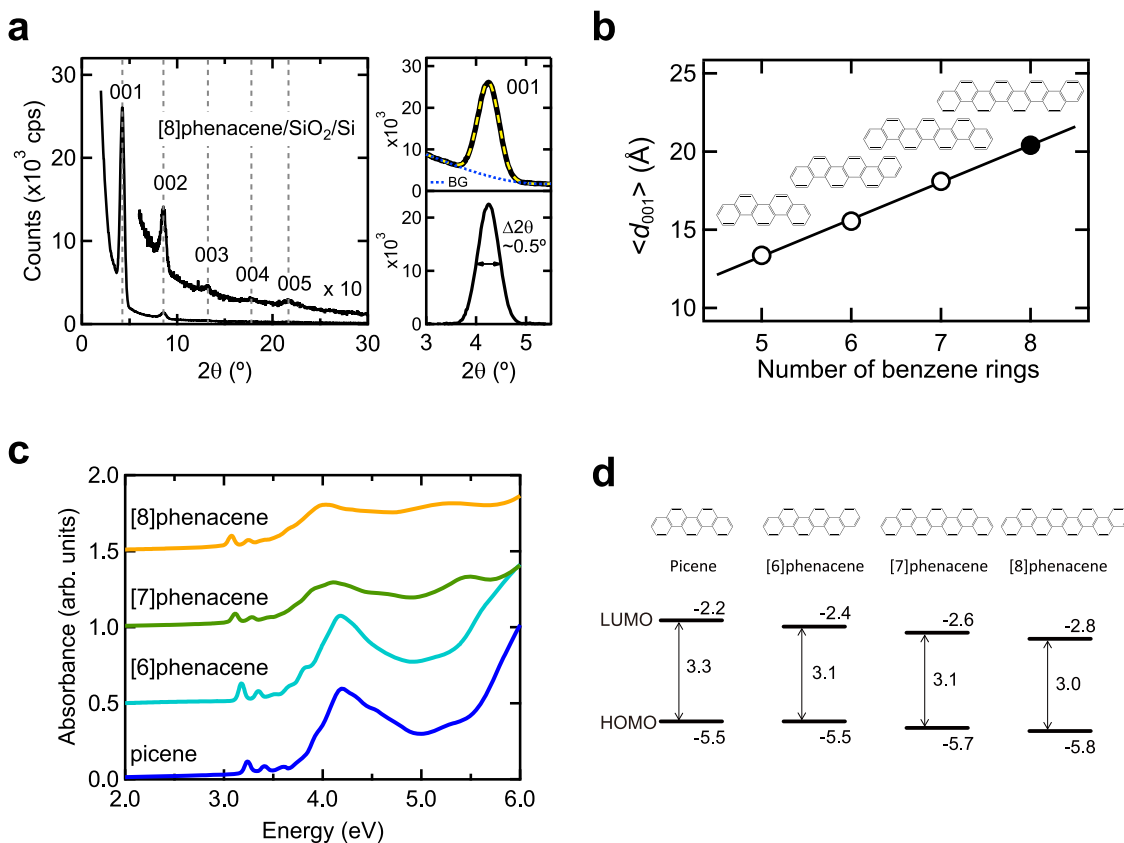


Figure 3 | (a) XRD pattern of [8]phenacene thin film on SiO_2/Si substrate. (b) $\langle d_{001} \rangle$ as a function of the number of benzene rings. (c) Absorption spectra of phenacene thin films and (d) energy diagrams of phenacene molecules.

4) and the van der Waals length of the long-axis of the molecule, 1.598 nm. Crystallite sizes are estimated to be 16.8(3) nm from the full width at half maximum (FWHM), $\Delta 2\theta \sim 0.5^\circ$, for (001) and (002) diffraction peaks with the Scherrer formula, as shown in Figure 3(a). The $\langle d_{001} \rangle$ value is plotted as a function of the number of benzene rings in phenacene molecules in Figure 3(b). This plot exhibits a clear linear relationship between the $\langle d_{001} \rangle$ and the number of benzene rings, or the length of phenacene molecules, which is clear evidence that the thin film is comprised of [8]phenacene molecules.

Furthermore, single crystals of [8] phenacene were grown, as is described in Supplementary Information, and the shape of the crystals (plate-like and transparent) is quite similar to that of other phenacene crystals^{9,10}, supporting the identity of [8]phenacene. The details of single-crystal preparation and a photograph of a single crystal are provided in Supplementary Information.

Electronic structure of [8]phenacene determined by absorption spectrum and photoelectron yield spectroscopy. The absorption spectrum of an [8]phenacene thin film is shown in Figure 3(c) together with other phenacene thin films. These spectra are quite similar to each other, confirming the identity of the [8]phenacene molecule. The optical gap corresponding to the gap between the highest occupied molecular orbital (HOMO) and the lowest unoccupied molecular orbital (LUMO) decreases as the number of benzene rings increases (3.3 eV for picene (five benzene rings) to 3.0 eV for [8]phenacene (eight benzene rings)). Photoelectron yield spectroscopy (PYS, not shown), indicates that the HOMO level of [8]phenacene, E_{HOMO} , is -5.8 eV. The energy diagram of [8]phenacene determined from its absorption spectrum (HOMO-LUMO gap) and PYS is shown in Figure 3(d), together with those of other

phenacene molecules; the energy diagrams for the phenacene molecules other than [8]phenacene are taken from references^{1,6,8,13}. As seen from Figure 3(d), [8]phenacene possesses a deep E_{HOMO} (-5.8 eV) and a wide band gap (3.0 eV). The energy diagram is quite similar to those for other phenacene molecules, although the band gap is slightly narrower and the E_{HOMO} is deeper with the increased number of benzene rings, implying that the [8]phenacene molecule has properties such as chemical stability and ease of hole-accumulation to the HOMO level, as in other phenacene molecules.

Field-effect transistor with thin film of [8]phenacene. Figure 4(a) displays the device structure of the [8]phenacene thin-film FET with an SiO_2 gate dielectric. 2,3,5,6-tetrafluoro-7,7,8,8-tetracyanoquinodimethane (F_4TCNQ) was inserted into the interface between the Au source/drain electrodes and the thin film. The absolute drain current ($|I_{\text{D}}|$) curves were plotted as a function of absolute gate voltage ($|V_{\text{G}}|$), as shown in Figure 4(b), where the drain voltage (V_{D}) was fixed at -100 V. From the $|I_{\text{D}}|^{1/2}$ vs. $|V_{\text{G}}|$ curves obtained at $V_{\text{D}} = -100$ V (not shown), the field-effect mobility μ and absolute threshold voltage $|V_{\text{TH}}|$ were evaluated using the metal-oxide-semiconductor (MOS) FET formula for the saturation regime²⁵. The μ , $|V_{\text{TH}}|$, and on-off ratio were estimated from the forward $|I_{\text{D}}|^{1/2}$ vs. $|V_{\text{G}}|$ plot (not shown) to be $1.74 \text{ cm}^2\text{V}^{-1}\text{s}^{-1}$, 51 V, and 5.6×10^6 , respectively, confirming clear p-channel FET characteristics. The output curves are shown in Figure 4(c). Clear saturation behaviours of $|I_{\text{D}}|$ in the high $|V_{\text{D}}|$ region, and the linear behaviours in the low $|V_{\text{D}}|$ region, were observed. No Schottky-like hole-injection barrier was present between the Au source/drain electrodes and the thin film in the low $|V_{\text{D}}|$ region owing to an insertion of F_4TCNQ . The μ value becomes >10 times as high as

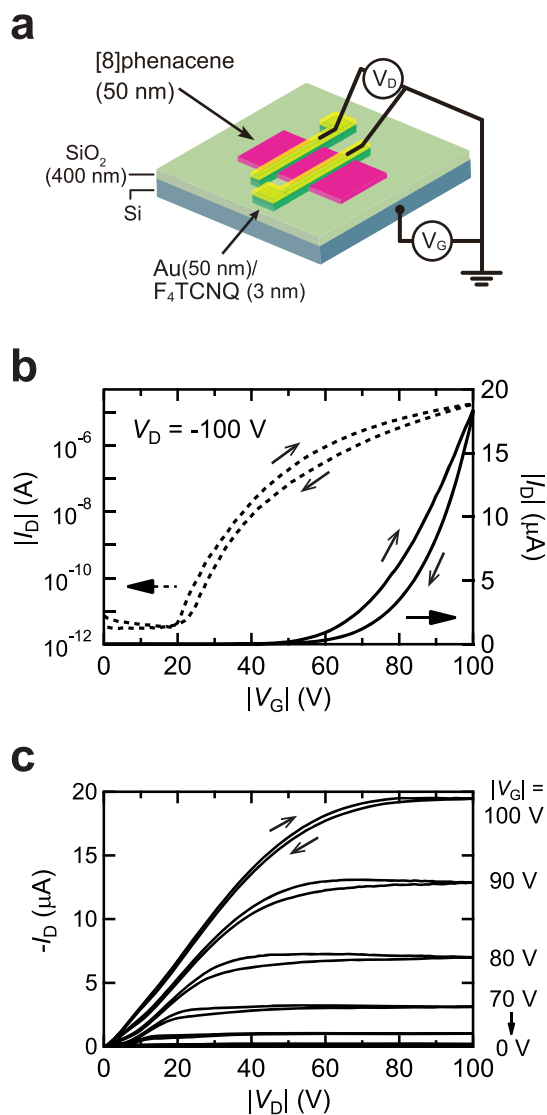


Figure 4 | (a) Device structure, (b) transfer and (c) output curves of [8]phenacene thin-film FET with SiO₂ gate dielectric. $W = 500 \mu\text{m}$ and $L = 450 \mu\text{m}$.

that, $1.4 \times 10^{-1} \text{ cm}^2 \text{ V}^{-1} \text{ s}^{-1}$, in FET devices without F₄TCNQ insertion, though only with an Au electrode. Thus, the F₄TCNQ insertion improves the [8]phenacene FET characteristics.

For a more precise presentation of device performance, the FET parameters (μ , $|V_{\text{th}}|$, on-off ratio and S) of five devices with SiO₂ fabricated in this study are listed in Table 1. The average values of their FET parameters are shown together with estimated standard deviation (e.s.d.). The average μ ($\langle \mu \rangle$) of $1.2(3) \text{ cm}^2 \text{ V}^{-1} \text{ s}^{-1}$ is quite favourable, suggesting the potential application of [8]phenacene in a practical FET.

Figure 5(a) shows a schematic representation of the [8]phenacene thin-film FET with a [1-butyl-3-methylimidazolium][hexafluorophosphate] (bmim[PF₆]) gate dielectric sheet (bmim[PF₆] sheet). This device is called an [8]phenacene thin-film EDL FET. The gate voltage is applied to the Au electrode that is connected to the bmim[PF₆] sheet, which can be regarded as a side-gate type structure. The transfer characteristic ($V_D = -1 \text{ V}$) of the [8]phenacene thin-film EDL FET device is shown in Figure 5(b). The μ , $|V_{\text{th}}|$, and on-off ratio were determined to be $16.4 \text{ cm}^2 \text{ V}^{-1} \text{ s}^{-1}$, 2.7 V and 1.7×10^6 from $|I_D|^{1/2}$ vs. $|V_G|$ plot of the forward transfer curve (Figure 5(b)).

The parameters of five EDL FETs fabricated in this study are listed in Table 2, showing values of $\langle \mu \rangle$ as high as $8(5) \text{ cm}^2 \text{ V}^{-1} \text{ s}^{-1}$. Furthermore, the average values of $|V_{\text{th}}|$ and S factors ($\langle |V_{\text{th}}| \rangle$ and $\langle S \rangle$) are as low as $2.5(2) \text{ V}$ and $0.2(1) \text{ V decade}^{-1}$, respectively. These values show that [8]phenacene thin-film EDL FET is an effective FET device, exhibiting both high mobility and low-voltage operation.

In a previous paper, we discussed the $|I_D|$ evolution when applying V_D and V_G as a function of time in a [7]phenacene thin-film FET with bmim[PF₆]²⁶. The $|I_D|$ gradually increases with increasing time and saturates above 1000 s. In the [7]phenacene thin-film EDL FET, the EDL capacitor was quickly formed in less than 2 s, but slow $|I_D|$ evolution was observed owing to the penetration of PF₆⁻ ions, i.e., the [7]phenacene thin-film FET is regarded as an electrochemical FET. However, as a bmim[PF₆] sheet was used in this [8]phenacene thin-film EDL FET, ion penetration may be neglected. In this case, the formation of an EDL capacitor was slower, and the large hysteresis seen in the transfer curves (Figure 5(b)) might originate from the slow motion of anions and cations in the sheet. The hysteresis decreased considerably in a long-duration scan of V_G , when the transfer curves were measured slowly (Figure 5(c)).

The output curves are shown in Figure 5(d). The $|I_D|$ increases linearly with increasing $|V_D|$, which means no Schottky-like hole-injection barrier between source/drain electrodes and the [8]phenacene thin film. This may be because the high density of hole-accumulation at the channel region results in destruction of the hole-injection barrier.

Discussion

We have synthesised an extended W-shaped hydrocarbon molecule, [8]phenacene, which consists of eight coplanar fused benzene rings. This synthetic route contains a sequence involving the Wittig reaction and the Mallory photocyclisation, which has been reported as a synthetic route to substituted π -extended-[n]phenacene derivatives ($n = 7, 11$)^{15,16,19}. We applied the above strategy to the synthesis of [8]phenacene with success. The present synthetic method (see Figure 2) only uses a simple repetition of the established reaction sequence (Wittig reaction-Mallory photocyclisation sequence) and because it can be used more easily than the previous one for the construction of larger phenacene frameworks¹⁷, it may become a practical and standard procedure to prepare non-substituted [n]phenacenes with $n > 8$. Thus, the synthetic route used here, the Mallory homologation strategy, is very powerful. This synthetic method can construct not only phenacene molecules with more than eight benzene rings, but also their substituted derivatives.

Table 1 | FET characteristics of [8]phenacene thin-film FETs with an SiO₂ dielectric

sample	μ (cm ² V ⁻¹ s ⁻¹)	$ V_{\text{th}} $ (V)	ON/OFF	S (V/decade)	L (μm)	W (μm)
#1	1.74	51.3	5.6×10^6	3.90	450	500
#2	1.30	34.5	1.0×10^6	4.40	350	500
#3	0.97	34.0	5.7×10^5	2.79	450	500
#4	1.01	35.4	5.4×10^5	3.70	450	500
#5	1.20	39.1	5.1×10^5	4.81	450	500
average	1.2(3)	39(7)	$2(2) \times 10^6$	3.9(8)		

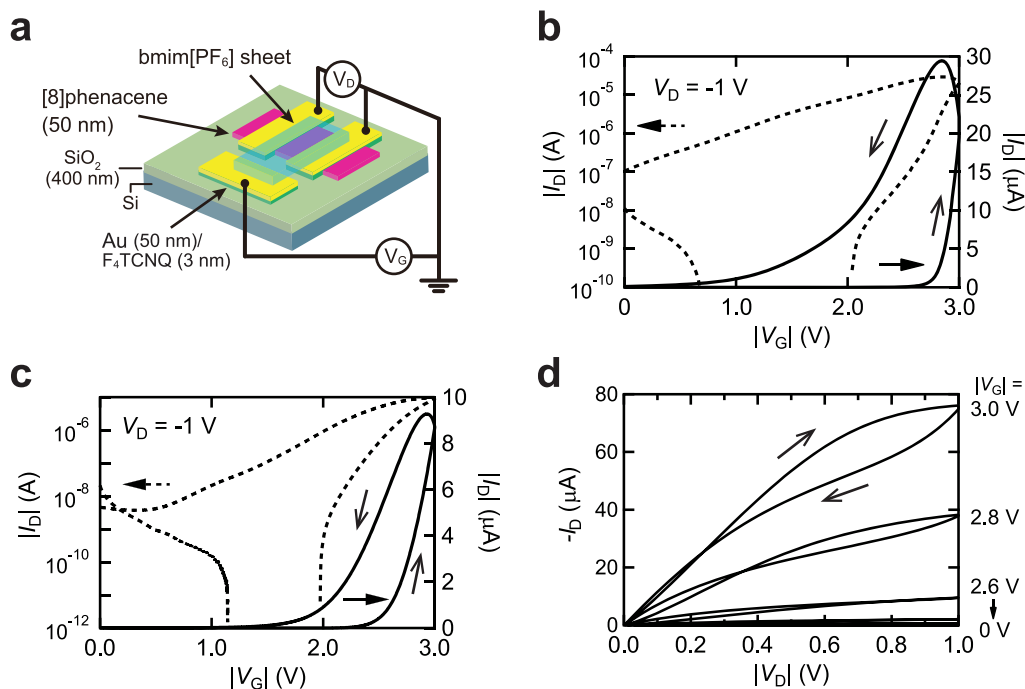


Figure 5 | (a) Device structure of an [8]phenacene thin-film EDL FET. Transfer curves in an [8]phenacene thin-film EDL FET measured with (b) quick and (c) slow scan of V_G . The quick scan was made with a hold time of 1 s; the slow scan with a hold time of 10 s. (d) Output curves for an [8]phenacene thin-film EDL FET measured with a quick scan of V_G . A $\text{bmim}[\text{PF}_6]$ polymer sheet was used as the EDL capacitor. $W = 900 \mu\text{m}$ and $L = 100 \mu\text{m}$.

We fabricated a thin-film transistor with [8]phenacene that had excellent p-channel FET characteristics such that μ reached $1.74 \text{ cm}^2 \text{ V}^{-1} \text{ s}^{-1}$ in a thin-film FET with an SiO_2 gate dielectric ($\langle \mu \rangle = 1.2(3) \text{ cm}^2 \text{ V}^{-1} \text{ s}^{-1}$) and $16.4 \text{ cm}^2 \text{ V}^{-1} \text{ s}^{-1}$ in an EDL FET with $\text{bmim}[\text{PF}_6]$ sheet ($\langle \mu \rangle = 8(5) \text{ cm}^2 \text{ V}^{-1} \text{ s}^{-1}$), values much higher than that reported previously in a patent¹⁷. The observation of p-channel characteristics is reasonable because of the high LUMO level shown in Figure 3(d), which is consistent with other phenacene molecules. The μ value (best $\mu = 1.74 \text{ cm}^2 \text{ V}^{-1} \text{ s}^{-1}$; $\langle \mu \rangle = 1.2(3) \text{ cm}^2 \text{ V}^{-1} \text{ s}^{-1}$) of the [8]phenacene thin-film FET with the SiO_2 gate dielectric is almost the same as those of thin-film FETs with picene ($1.4 \text{ cm}^2 \text{ V}^{-1} \text{ s}^{-1}$)^{1,2} and [7]phenacene ($0.75 \text{ cm}^2 \text{ V}^{-1} \text{ s}^{-1}$)⁸, while it is lower than that ($7.4 \text{ cm}^2 \text{ V}^{-1} \text{ s}^{-1}$) of the [6]phenacene thin-film FET. On the other hand, the μ value (best $\mu = 16.4 \text{ cm}^2 \text{ V}^{-1} \text{ s}^{-1}$; $\langle \mu \rangle = 8(5) \text{ cm}^2 \text{ V}^{-1} \text{ s}^{-1}$) of the [8]phenacene thin-film EDL FET is much higher than that ($0.28 \text{ cm}^2 \text{ V}^{-1} \text{ s}^{-1}$) of the [7]phenacene thin-film EDL FET²⁶, while no data have been reported for EDL FETs with thin films of picene and [6]phenacene.

Here it is important to discuss the reason why the μ of the [8]phenacene thin-film EDL FET is very high. We may note the roughness of thin-film of [8]phenacene (rms roughness = 1.7 nm), and its greater flatness than other phenacenes as described in the Results section. As the EDL capacitor is formed on the thin film (see Figure 5(a)), the flatness may significantly affect the FET performance. If this is the case, the high μ in the [8]phenacene thin-film EDL

FET may be reasonably explained. However, further study is necessary to clarify the origin of the high μ , and detailed experiments on the correlation between flatness and μ in phenacene EDL FETs may be indispensable. Moreover, other factors such as differences in the packing of molecules and electronic structures must be investigated. In this study, [8]phenacene was shown to be suitable for FET application. This study thus not only clarified an effective synthetic route to [8]phenacene, and its physical properties, but also produced a high-performance [8]phenacene thin-film FET. This may inspire the synthesis of more extended phenacene systems.

Methods

Materials. The synthetic route is shown in Figure 2, and reaction steps are described in Synthetic Protocol in Results. The experimental details are described in this section (intermediates 8–10 and [8]phenacene) and Supplementary Information (intermediate 4, 5 and 6).

1-Phenanthrenecarbaldehyde 8. A solution of 1-(bromomethyl)phenanthrene 7¹⁹ (890 mg, 3.28 mmol) and hexamethylenetetramine (552 mg, 3.24 mmol) in CHCl_3 (15 ml) was refluxed for 1.5 h. The solvent was evaporated under reduced pressure and the residue was dissolved in a mixture of acetic acid (AcOH, 3 ml) and water (3 ml) and heated at $\sim 100^\circ\text{C}$ for 1 h. After cooling to room temperature, the mixture was extracted with CH_2Cl_2 (20 ml) and the extract was washed successively with water and NaHCO_3 aqueous solution, and dried over MgSO_4 . The solvent was evaporated under reduced pressure and the residue was chromatographed (silica gel, CH_2Cl_2) to afford 1-phenanthrenecarbaldehyde 8 [(605 mg, yield of 89%), mp $106\text{--}106.5^\circ\text{C}$ (lit²⁷, $110.5\text{--}111.5^\circ\text{C}$)]. The NMR spectral features (Figure S7) and mp of the obtained aldehyde 8 were identical to those previously published^{27,28}.

Table 2 | FET characteristics of [8]phenacene thin-film FETs with a $\text{bmim}[\text{PF}_6]$ gate dielectric sheet

sample	μ ($\text{cm}^2 \text{ V}^{-1} \text{ s}^{-1}$)	$ V_{th} $ (V)	ON/OFF	S (V/decade)	L (μm)	W (μm)
#1	16.40	2.74	2.0×10^7	0.12	100	900
#2	7.07	2.41	6.2×10^6	0.11	100	200
#3	11.04	2.35	6.7×10^6	0.18	100	173
#4	4.89	2.59	8.9×10^6	0.21	100	545
#5	3.06	2.59	5.0×10^3	0.36	100	212
average	8(5)	2.5(2)	$8(7) \times 10^6$	0.2(1)		



[8]phenacene. To a solution of phosphonium salt **6** (103 mg, 0.50 mmol) and aldehyde **8** (293 mg, 0.50 mmol) in CH_2Cl_2 (20 ml) was added a solution of KOH (0.2 g in 0.2 ml of H_2O) and the mixture was stirred at rt for 2 h. The precipitate formed was collected and successively washed with EtOH and toluene to afford chrysenylphenanthrylene **9** (133 mg, 62%, crude containing *E*- and *Z*-isomers). The crude product was used in the following photoreaction without further separation and purification.

The crude chrysenylphenanthrylene **9** (75 mg, 0.17 mmol) was dissolved in 500 ml of toluene and I_2 (4.5 mg, 0.02 mmol) was added. The solution was purged with air and irradiated as described for the synthesis of 1-methylchrysene **4**. The precipitate formed was collected. The crude product was refluxed in 20 ml of $\text{CHCl}_2\text{CHCl}_2$ for 8 h. After cooling to room temperature, [8]phenacene was collected as pale yellow powder [21 mg, yield of 28%, mp > 300°C]. Solid-state CP-MAS ^{13}C NMR spectrum shown in Figure 1(b) (Details are described in the section 'Solid state CP-MAS NMR analysis'). To facilitate comparison of the CP-MAS ^{13}C NMR spectra of intermediate **9** and [8]phenacene, both are shown in Figure S9 of Supplementary Information.

IR (neat): $\nu_{\text{max}} = 3047, 1283, 1136, 1028, 943, 864, 804, 771, 740, 692, 610, 579, 536$ and 523 cm^{-1} . MALDI-TOF MS and elemental analysis are described in the section 'Characterisation by Energy Dispersive x-ray Spectroscopy, Mass spectrum and Elemental Analysis'. The CP-MAS NMR and MALDI-TOF MS were measured using VARIAN NMR SYSTEM 600 MHz spectrometer and Bruker Autoflex mass spectrometer, respectively.

Chrysenylphenanthrylene 10. To establish that intermediate **9** is chrysenylphenanthrylene, which is an important intermediate in the reaction sequence leading to [8]phenacene, chrysenylphenanthrylene **10** was synthesised using the following synthetic route, *via* catalytic hydrogenation. A crude mixture of product **9** (18 mg, 42 μmol) and 10% Pd/C (5 mg) was added to 100 ml of *N,N*-dimethylformamide (DMF). The mixture was heated at 100°C under a hydrogen stream for 2 h. After cooling to rt., Pd/C was filtered off and the solvent was removed under reduced pressure. The residue was washed with methanol to afford chrysenylphenanthrylene **10** [14 mg, yield of 77%], and recrystallisation from a toluene/ethanol solution containing **10** yielded colourless crystals [mp 291.5–293°C].

^1H NMR of **10** (CDCl_3 , 600 MHz, 40°C): $\delta_{\text{H}} = 8.81$ (d, 1H, $J = 8.3$ Hz), 8.75–8.80 (2H, two doublets overlapped), 8.72–8.76 (2H, two doublets overlapped), 8.65 (d, 1H, $J = 8.4$ Hz), 8.35 (d, 1H, $J = 9.3$ Hz), 8.12 (d, 1H, $J = 9.2$ Hz), 8.00–8.04 (2H, two doublets overlapped), 7.92 (d, 1H, $J = 7.3$ Hz), 7.82 (d, 1H, $J = 9.2$ Hz), 7.73 (ddd, 1H, $J = 8.3, 7.2, 1.2$ Hz), 7.60–7.70 (m, 4H), 7.58 (t, 1H, $J = 7.3$ Hz), 7.46–7.49 (2H, two doublets overlapped), 3.67 (m, 4H).

^{13}C NMR of **10** (CDCl_3 , 150 MHz, 40°C): $\delta_{\text{C}} = 138.82, 138.78, 132.4, 131.9, 131.3, 131.2, 131.1, 130.8, 130.7, 130.4, 129.1, 128.71, 128.65, 128.1, 127.6, 127.4, 127.2, 127.1, 126.9, 126.8, 126.7, 126.6, 126.5, 126.4, 123.3, 123.0, 122.6, 122.0, 121.8, 121.52, 121.46, 35.0$. IR ν_{max} (neat): 800, 772, 740 cm^{-1} . FAB HRMS: experimental $m/z = 433.1936$ [$\text{C}_{34}\text{H}_{25}^+$: (**10** + H^+)], consistent with the calculated m/z (433.1956) for $\text{C}_{34}\text{H}_{25}^+$. Anal. Calcd. for **10** ($\text{C}_{34}\text{H}_{24}$): C, 94.41%; H, 5.59%. Found C, 94.19%; H, 5.57%.

The ^1H NMR spectrum of **10** in the aromatic region (see Figure S8) can be analysed by superposition of the resonance signals of 1-methylphenanthrene²⁹ and 1-methylchrysene²⁹, as is predicted from the molecular structure of **10**. Furthermore, the HRMS and elemental analysis also confirmed the successful synthesis of **10**. Thus, all the results (NMR, HRMS and elemental analysis) supporting the synthesis of product **10** guarantee that intermediate **9** is in fact chrysenylphenanthrylene, because product **10** can be prepared only by the hydrogenation of chrysenylphenanthrylene, as shown in Figure 2.

Characterisation of [8]phenacene sample and thin film. Optical absorption was recorded with a UV-VIS absorption spectrometer (JASCO V-670 iRM EX). Photoelectron yield spectroscopy was performed using an ionization energy measurement system (Bunkoukeiki Co., Ltd.) to determine the energy of the HOMO level. The surface morphology and the crystallite size of the [8]phenacene thin film were investigated by AFM and XRD. The AFM image and XRD pattern were measured with an AFM measurement system (SII Nano Technology SPA400) and an X-ray diffractometer (Rigaku Smartlab-pro), respectively.

FET device fabrication. A 50 nm thick film of [8]phenacene was formed on the SiO_2/Si substrate by thermal deposition under 10^{-7} Torr, to produce the device in which SiO_2 was used as the gate dielectric. The surface of the SiO_2/Si substrate was coated with hexamethyldisilazane (HMDS) to produce a hydrophobic surface. The thickness of the Au source/drain electrodes was 50 nm. 3 nm thick F_4TCNQ was inserted into the space between the Au electrodes and the thin film to reduce contact resistance. The Au source/drain electrodes and the F_4TCNQ were replaced by thermal deposition at 10^{-7} Torr.

The capacitances per area, C_0 , for SiO_2 (400 nm) and C_{EDL} for the EDL capacitor of bmim[PF₆] sheet were measured using a precision LCR meter (Agilent E4980A), showing C_0 and C_{EDL} values of 8.07 nF cm^{-2} and 3.99 $\mu\text{F cm}^{-2}$, respectively. The fabrication of the bmim[PF₆] sheet is described in Supplementary information, and a photo of the sheet is shown in Figure S3 in Supplementary information. The C_0 and C_{EDL} were determined by extrapolation of the capacitance measured at 20 Hz–1 kHz to 0 Hz; the C_{EDL} is twice the capacitance per area of sheet because of the formation of two EDL capacitors. The channel width W and the length L for each device are indicated in figure captions. The μ values were determined from the forward transfer curves in the saturation regime with the general MOS formula²⁵. The FET characteristics were recorded using a semiconductor parametric analyser (Agilent B1500A)

in an Ar-filled glove box. As seen in the device structures, the source electrode was grounded ($V_S = 0$). Negative voltage was applied to V_G and V_D in measurements of transfer and output curves.

- Okamoto, H. *et al.* Air-assisted high-performance field-effect transistor with thin films of picene. *J. Am. Chem. Soc.* **130**, 10470–10471 (2008).
- Kawasaki, N., Kubozono, Y., Okamoto, H., Fujiwara, A. & Yamaji, M. Trap states and transport characteristics in picene thin film field-effect transistor. *Appl. Phys. Lett.* **94**, 043310-1–043310-3 (2009).
- Lee, X. *et al.* Quantitative analysis of O_2 gas sensing characteristics of picene thin film field-effect transistors. *Org. Electron.* **11**, 1394–1398 (2010).
- Kaji, Y. *et al.* Low voltage operation in picene thin film field-effect transistor and its physical characteristics. *Appl. Phys. Lett.* **95**, 183302-1–183302-3 (2009).
- Sugawara, Y. *et al.* O_2 -exposure and light-irradiation properties of picene thin film field-effect transistor: A new way toward O_2 gas sensor. *Sensors and Actuators B* **171–172**, 544–549 (2012).
- Komura, N. *et al.* Characteristics of [6]phenacene thin film field-effect transistor. *Appl. Phys. Lett.* **101**, 083301-1–083301-4 (2012).
- Eguchi, R. *et al.* Fabrication of high performance/highly functional field-effect transistor devices based on [6]phenacene thin films. *Phys. Chem. Chem. Phys.* **15**, 20611–20617 (2013).
- Sugawara, Y. *et al.* Characteristics of field-effect transistors using the one-dimensional extended hydrocarbon [7]phenacene. *Appl. Phys. Lett.* **98**, 013303-1–013303-3 (2011).
- Kawai, N. *et al.* Characteristics of single crystal field-effect transistors with a new type of aromatic hydrocarbon, picene. *J. Phys. Chem. C* **116**, 7983–7988 (2012).
- He, X. *et al.* Fabrication of single crystal field-effect transistors with phenacene-type molecules and their excellent transistor characteristics. *Org. Electron.* **14**, 1673–1682 (2013).
- He, X. *et al.* Systematic control of hole-injection barrier height with electron acceptors in [7]phenacene single-crystal field-effect transistors. *J. Phys. Chem. C* **118**, 5284–5293 (2014).
- Okamoto, H. *et al.* Facile synthesis of picene from 1,2-di(1-naphthyl)ethane by 9-fluorenoen-sensitized photolysis. *Org. Lett.* **13**, 2758–2761 (2011).
- Kubozono, Y. *et al.* Metal-intercalated aromatic hydrocarbons: a new class of carbon-based superconductors. *Phys. Chem. Chem. Phys.* **13**, 16476–16493 (2011).
- Nishihara, Y. *et al.* Phenanthro[1,2-*b*:8,7-*b'*]dithiophene: a new picene-type molecule for transistor applications. *RSC Adv.* **3**, 19341–19347 (2013).
- Mallory, F. B., Butler, K. E., Evans, A. C. & Mallory, C. W. Phenacenes: a family of graphite ribbons. 1. Syntheses of some [7]phenacenes by stilbene-like photocyclizations. *Tetrahedron Lett.* **37**, 7173–7176 (1996).
- Mallory, F. B. *et al.* Phenacenes: a family of graphite ribbons. 2. Syntheses of some [7]phenacenes and an [11]phenacene by stilbene-like photocyclizations. *J. Am. Chem. Soc.* **119**, 2119–2124 (1997).
- Nakatsuka, M. inventors; Yamamoto Chemicals Inc. assignee. Yuuki-toranjisu. Japan Patent, JP5378690B2. 2013 October 4.
- Watanabe, M. *et al.* The synthesis, crystal structure and charge-transport properties of hexacene. *Nature Chem.* **4**, 574–578 (2012).
- Mallory, F. B. *et al.* Phenacenes: a family of graphite ribbons. Part 3: Iterative strategies for the synthesis of large phenacenes. *Tetrahedron* **57**, 3715–3724 (2001).
- Angaly, S. J. The Sommelet Reaction. *Org. React.* **8**, 197–217 (1954).
- Mallory, F. B. & Mallory, C. W. Photocyclization of stilbenes and related molecules. *Org. React.* **30**, 1–456 (1984).
- Okamoto, H. *et al.* Efficient synthetic photocyclization for phenacenes using a continuous flow reactor. *Chem. Lett.* in press (2014).
- De, A., Ghosh, R., Roychowdhury, S. & Roychowdhury, P. Structural analysis of picene, $\text{C}_{22}\text{H}_{14}$. *Acta Crystallogr. C* **41**, 907–909 (1985).
- Mitsuhashi, R. *et al.* Superconductivity in alkali-metal-doped picene. *Nature* **464**, 76–79 (2010).
- Sze, S. M. *Semiconductor devices, Physics and Technology* (John Wiley & Sons, Inc, 2002).
- Kaji, Y. *et al.* Characteristics of conjugated hydrocarbon based thin film transistor with ionic liquid gate dielectric. *Org. Electron.* **12**, 2076–2083 (2011).
- Bachmann, W. E. & Boatner, C. H. Phenanthrene derivatives. V. The Beckmann rearrangement of the oximes of acetylphenanthrenes and benzoylphenanthrenes. *J. Am. Chem. Soc.* **58**, 2097–2101 (1936).
- Pampin, M. C., Estévez, J. C., Estévez, R. J., Maestrob, M. & Castedo, L. Heckmann-mediated synthesis and photochemically induced cyclization of [2-(2-styrylphenyl)ethyl]carbamic acid ethyl esters and 2-styryl-benzoic acid methyl esters: total synthesis of naphtho[2,1-f]isoquinolines (2-azachrysens). *Tetrahedron* **59**, 7231–7243 (2003).
- Paul, S., Jana, R. & Ray, J. K. Palladium-catalyzed intramolecular C-H activation: a synthetic approach towards polycyclic aromatic hydrocarbons. *Synlett* **10**, 1463–1468 (2010).

Acknowledgments

The authors wish to express their gratitude to Mr. Yuma Shimo and Mr. Kazuya Teranishi for their kind assistance in the preparation of single crystals of [8]phenacene. This study was



partly supported by Grants-in-aid (23684028, 22244045, 24654105, 24550054) from MEXT, by the program to disseminate the tenure tracking system of the Japan Science and Technology Agency (JST), by the LEMSUPER project (JST EU Superconductor Project), and the JST ACT-C project, and by the Program for Promoting the Enhancement of Research Universities.

Author contributions

H.O. and Y.K. designed this research project and supervised experiments. H.O. and S.G. performed the synthesis and characterisation of the [8]phenacene sample. R.E., S.H. and H.G. carried out FET work and characterisation of thin films. K.G., Y.S., M.I. and Y.T. dealt with solid-state NMR, XRD, EDX, MALDI-TOF MS, respectively. H.O. and R.E. wrote the sections on synthesis and FET work in this paper, respectively. Y.K. managed (edited) all parts of this paper.

Additional information

Supplementary information accompanies this paper at <http://www.nature.com/scientificreports>

Competing financial interests: The authors declare no competing financial interests.

How to cite this article: Okamoto, H. *et al.* An Extended Phenacene-type Molecule, [8]Phenacene: Synthesis and Transistor Application. *Sci. Rep.* **4**, 5330; DOI:10.1038/srep05330 (2014).



This work is licensed under a Creative Commons Attribution-NonCommercial-NoDerivs 4.0 International License. The images or other third party material in this article are included in the article's Creative Commons license, unless indicated otherwise in the credit line; if the material is not included under the Creative Commons license, users will need to obtain permission from the license holder in order to reproduce the material. To view a copy of this license, visit <http://creativecommons.org/licenses/by-nc-nd/4.0/>